Trenton Cathcart
Date: 11/15/2023

LabVIEW-based Servo Integration and Modeling

Table of Contents

I. List of Tables: 1
II. List of Figures: 1
III. Objectives: 1
IV. Equipment Used: 2
V. Background Theory: 2
VI. Preliminary Calculations: 3
VII. Procedure/Result/Analysis: 3
- **I. Configuring a LabVIEW VI for the QUBE-Servo 2:** 3
- **II. Measuring Speed Using the Encoder:** 5
- **III. Stability: Analyzing System Stability with VI Models:** 8
- **IV. Bump Test Modeling:** 9
- **V. First Principles Modeling:** 12

VIII. Conclusion: 14

I. List of Tables:

A. N/A

II. List of Figures:

A. Figure 1: 1 Full Rotation in Counts
B. Figure 2: Full Rotation in Degrees
C. Figure 3: Driving the DC Motor
D. Figure 4: Encoder Response with No Filter (2.4)
E. Figure 5: Encoder Response with a Filter (2.7)
F. Figure 6: Cutoff Frequency at 10 rad/s (2.9)
G. Figure 7: Cutoff Frequency at 50 rad/s (2.9)
H. Figure 8: Cutoff Frequency at 200 rad/s (2.9)
I. Figure 9: (3.1)
J. Figure 10: (3.3)
K. Figure 11: Block Diagram for Bump Test Modeling
L. Figure 12: Plot for Steady-State Gain (4.3)
M. Figure 13: Plot for Time Constant (4.4)
N. Figure 14: Test for New Gain and Time Constant (4.5)
O. Figure 15: Response for New Block Diagram (5.4)
P. Figure 16: Response for Differential Equation (5.5)

III. Objectives:

The objective for Experiment 8 in the Control Systems Lab was to create a LabVIEW model using QUARC blocks to drive a DC motor and measure its angular position or speed. The experiment involved designing a model that measures the servo velocity and analyzing the response of the angular velocity to determine the gain and time constants for the equipment used. This allowed the students to create a detailed transfer function that models the system, enabling them to compare the theoretical and actual responses in real time.

IV. Equipment Used:

- Labview
- Quarc Software
- Qube-2 Servo
- Computer

V. Background Theory:

The background theory for Experiment 8 centers on the integration and modeling of a QUBE-Servo 2 system using LabVIEW and QUARC blocks. The QUBE-Servo 2, a rotary servo system, features a DC motor connected to a PWM amplifier. Its angular position or speed is measured using encoders, which are devices that convert the angular position or motion of a shaft or axle to an analog or digital signal. The QUBE-Servo 2 system employs an incremental optical encoder, which generates signals as the shaft rotates. These signals are then processed to determine the angular position.

A key aspect of the system is the back-emf voltage, which is dependent on the motor's speed and the back-emf constant. This voltage plays a critical role in the motor's functioning, opposing the current flow and affecting the motor's performance. Kirchhoff's Voltage Law is used to relate the motor voltage, resistance, current, and back-emf, providing a foundation for understanding the motor's electrical behavior.

The experiment also delves into the theory of filtering, specifically the use of low-pass filters to block high-frequency signal components. This is crucial for ensuring accurate signal processing and measurement. The stability of the system is analyzed using Bounded-Input Bounded-Output (BIBO) principles and pole analysis, determining whether every bounded input yields a bounded output, which is a fundamental aspect of system stability.

In summary, the background theory for this experiment encompasses the operational principles of the QUBE-Servo 2 system, including its electrical and mechanical components, the role of encoders in measuring angular position, the significance of back-emf voltage, and the application of filtering and stability analysis techniques. This theoretical foundation is essential for understanding the system's behavior and for designing effective control models using LabVIEW and QUARC blocks.

VI. Preliminary Calculations:

No Preliminary calculations required.

VII. Procedure/Result/Analysis:

I. Configuring a LabVIEW VI for the QUBE-Servo 2:

In Part 1 of Experiment 8, we focused on configuring a LabVIEW Virtual Instrument (VI) for the QUBE-Servo 2, using the Quanser Rapid Control Prototyping Toolkit blocks. Our main task was to drive the DC motor and measure its corresponding angle. Initially, we configured the QUBE-Servo motor to read the encoder and drive the DC motor in LabVIEW. This setup was essential for the subsequent steps of the experiment.

$$Gain = \frac{counts}{360} = \frac{2039}{360} = 0.176557$$

During this process, we observed and documented key aspects of the system's operation. In **Figure 1**, titled "1 Full Rotation in Counts," we captured the encoder's output as it measured a full rotation of the motor in count units. This figure was crucial in demonstrating the encoder's precision in measuring the angular position of the motor. Next, in **Figure 2**, "Full Rotation in Degrees," we converted these counts into degrees. This conversion provided a more comprehensible representation of the motor's rotational movement, making it easier to interpret the data.

Lastly, **Figure 3**, "Driving the DC Motor," showcased our control of the DC motor's angular position via the LabVIEW VI. This figure was instrumental in illustrating how the motor was driven and its position measured, demonstrating the practical application of our configuration in the LabVIEW environment.

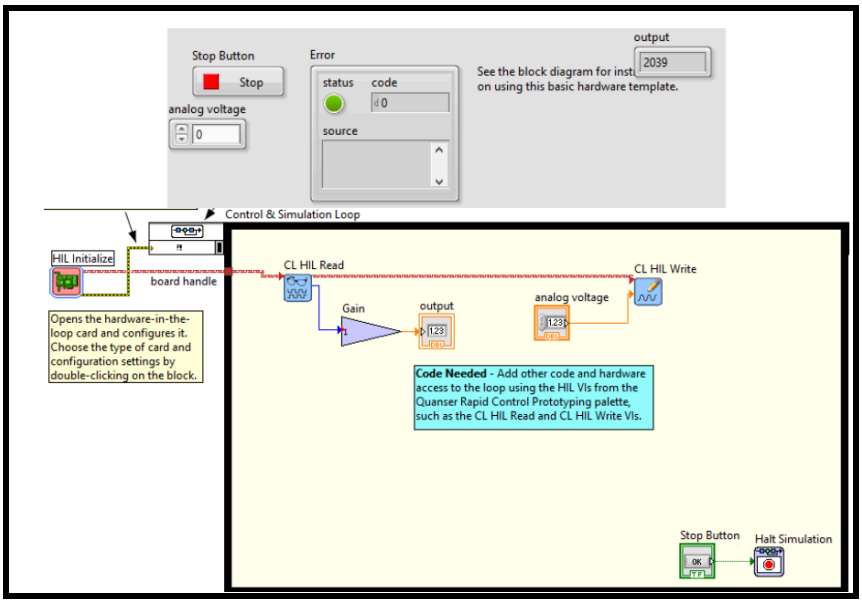

Figure 1: Full Rotation in Counts

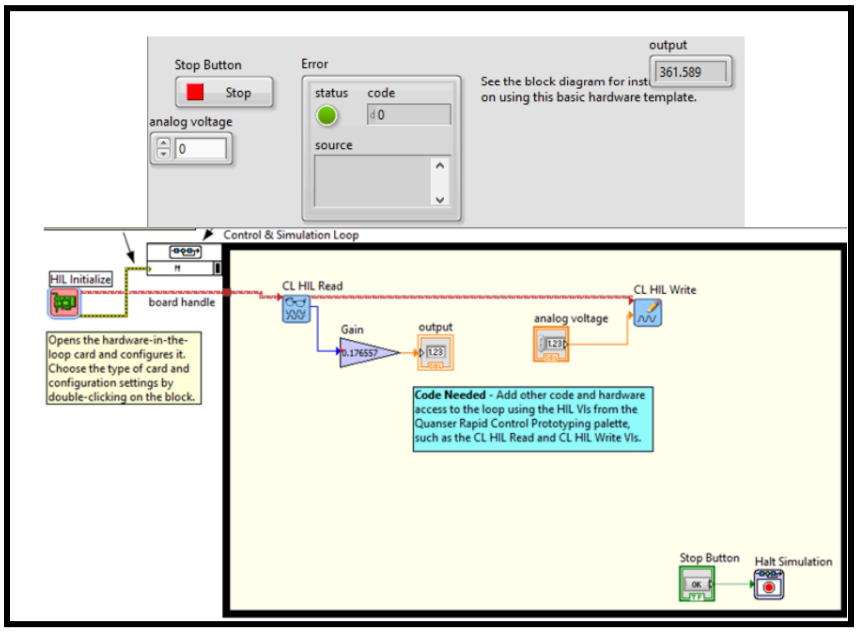

Figure 2: Full Rotation in Degrees

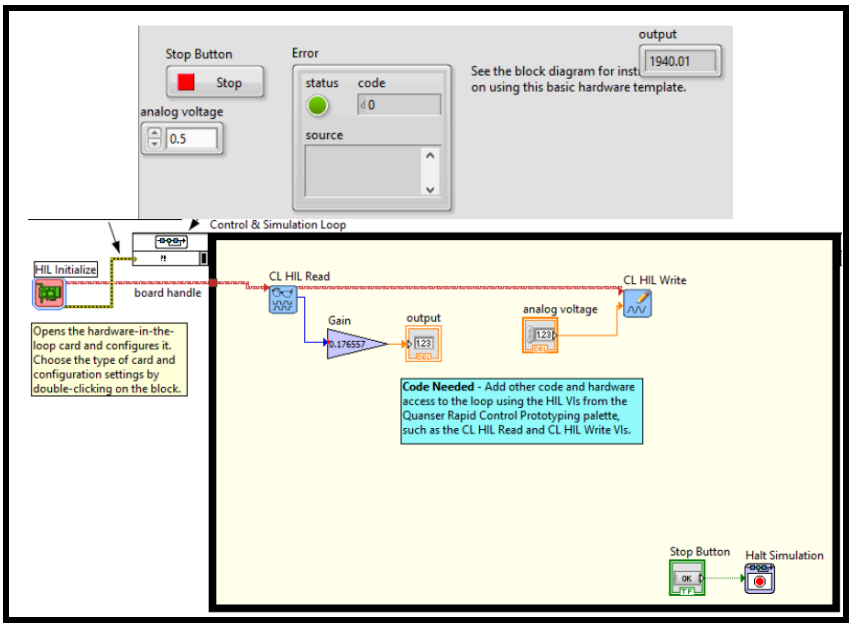

Figure 3: Driving the DC Motor

II. Measuring Speed Using the Encoder:

In Part 2, our focus was on enhancing the measurement of servo velocity using the encoder by applying a low-pass filter to the data. Initially, we adjusted the LabVIEW Virtual Instrument (VI) from the first part to measure the gear position in radians instead of degrees. This modification was crucial for obtaining more precise speed measurements.

$$Gain = Position\ in\ Degrees * \frac{\pi}{180} = 0.176557 * \frac{\pi}{180} = 0.0030815$$

We then observed the encoder speed response without any filtering, as depicted in **Figure 4.** This unfiltered response revealed a significant level of noise, highlighting the need for a low-pass filter. To address this, we introduced a low-pass filter into our VI. The effect of the filter was immediately noticeable, as seen in **Figure 5**, where the encoder's speed response showed a marked improvement in clarity.

Further refinement was achieved by experimenting with different cutoff frequencies for the low-pass filter. We observed the effects of these variations in **Figure 6** at 10 rad/s, **Figure 7** at 50 rad/s, and **Figure 8** at 200 rad/s. These figures demonstrated the impact of the filter's cutoff frequency on the encoder's speed response, helping us understand the balance between signal clarity and response sharpness.

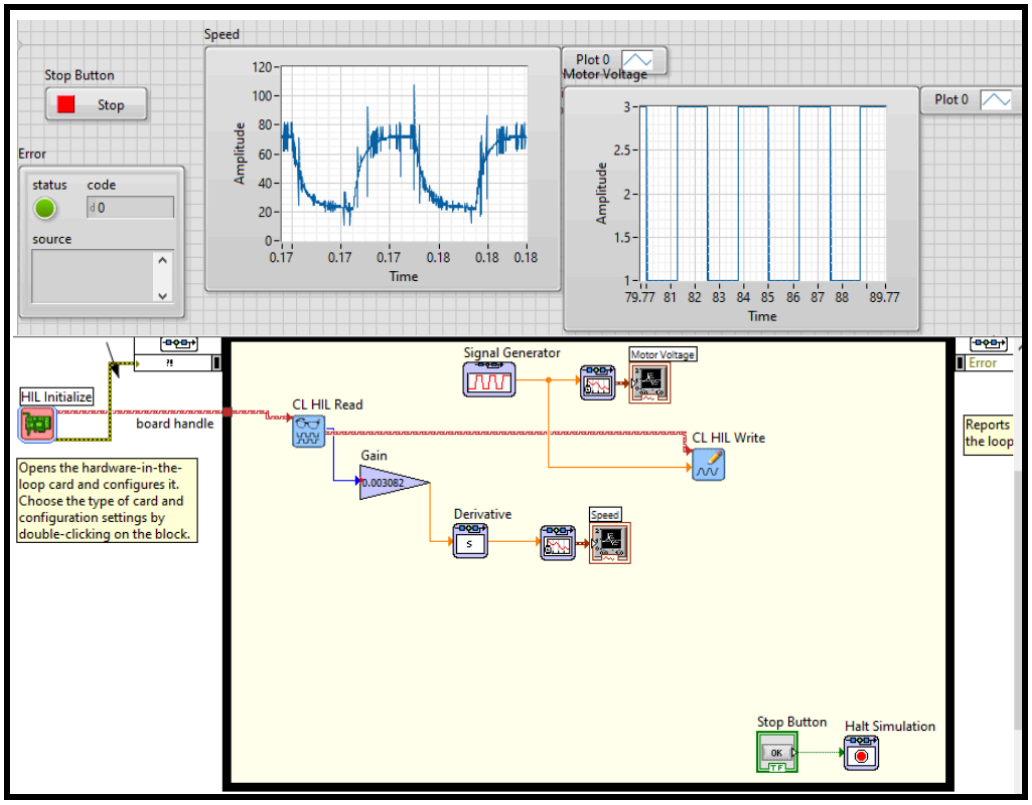

Figure 4: Encoder Response with No Filter (2.4)

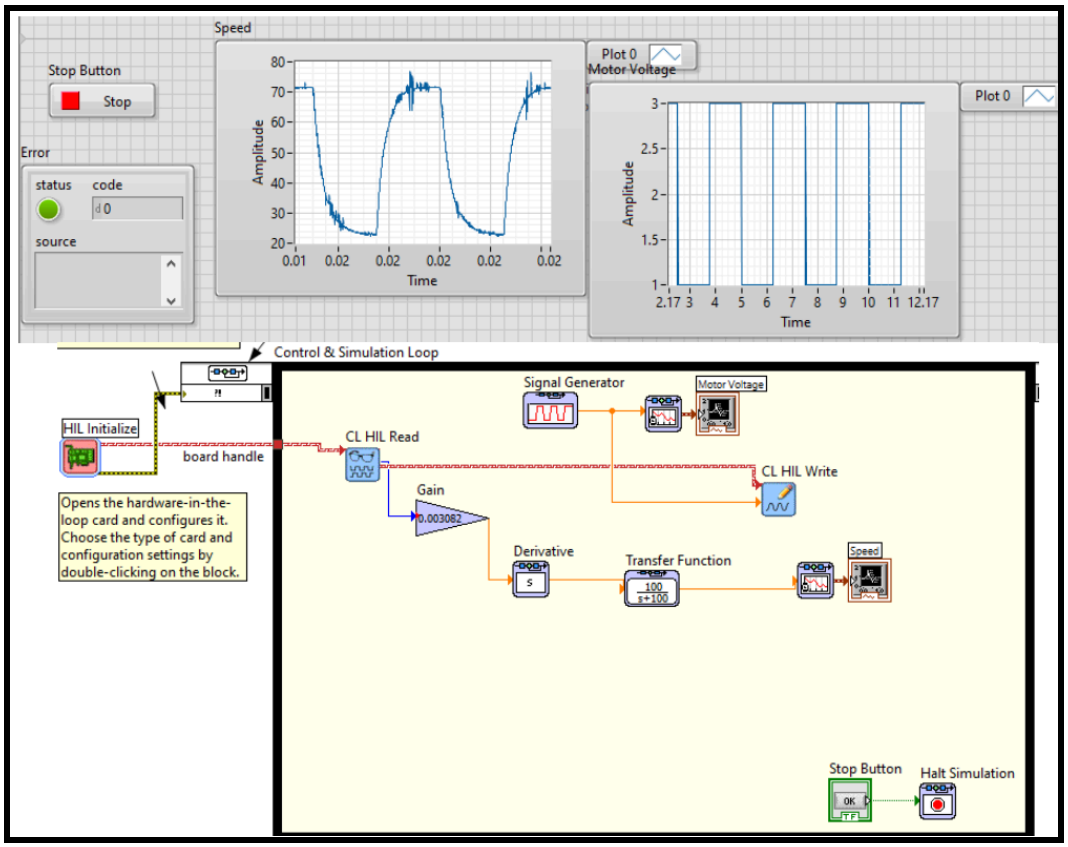

Figure 5: Encoder Response with a Filter (2.7)

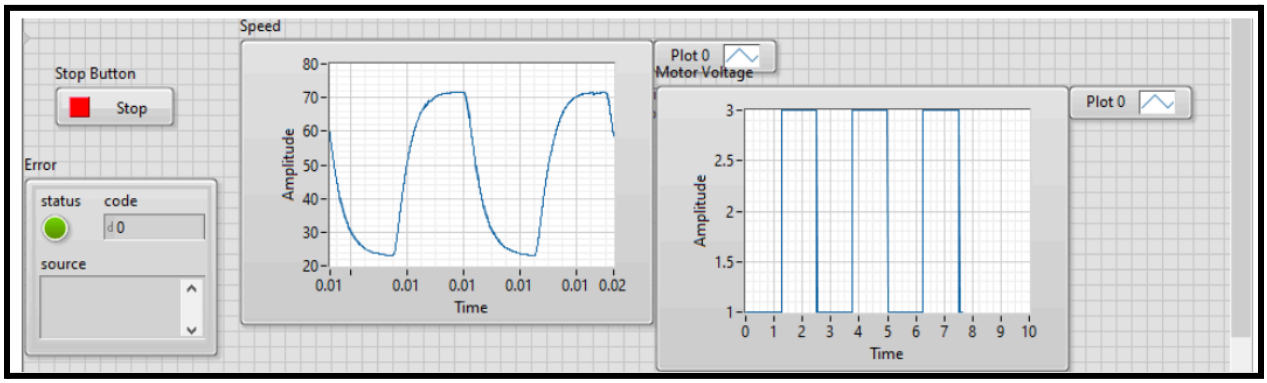

Figure 6: Cutoff Frequency at 10 rad/s (2.9)

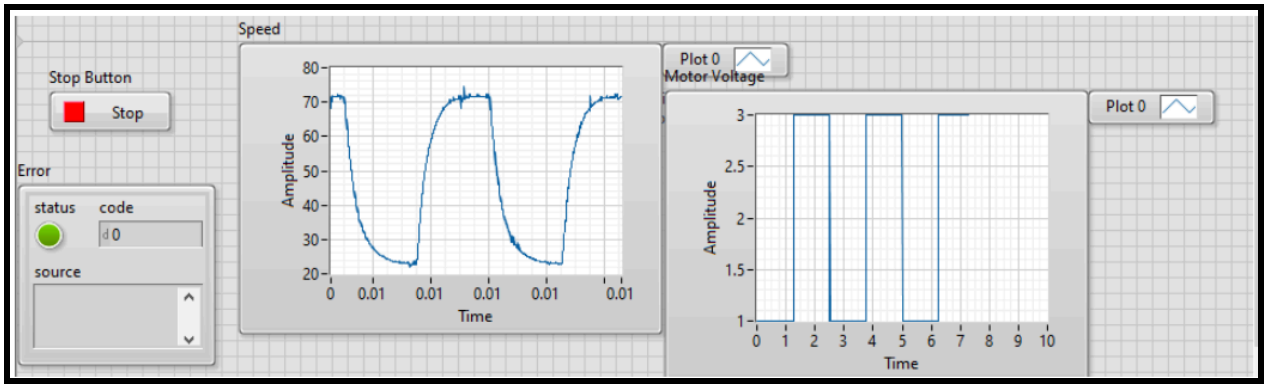

Figure 7: Cutoff Frequency at 50 rad/s (2.9)

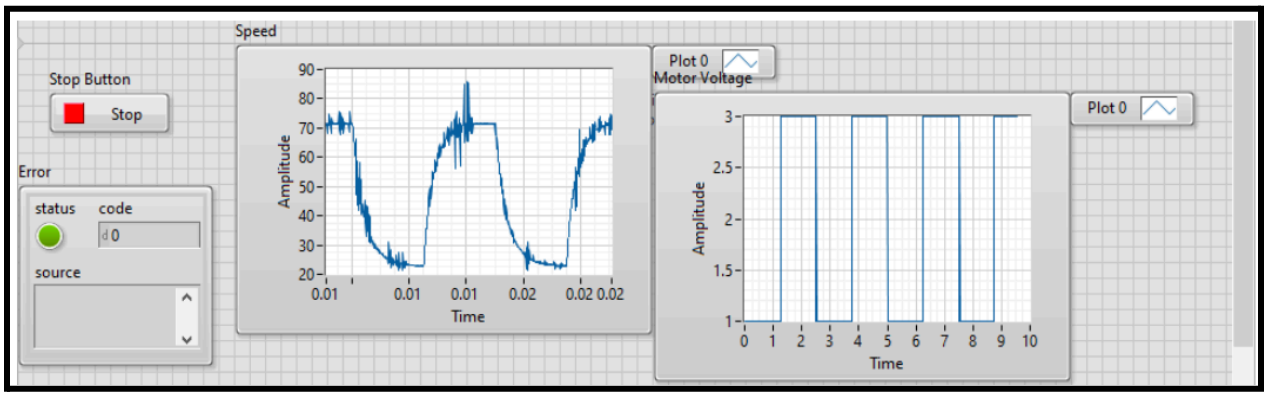

Figure 8: Cutoff Frequency at 200 rad/s (2.9)

III. Stability: Analyzing System Stability with VI Models:

In Part 3 of Experiment, we built upon the previously designed models to develop a LabVIEW Virtual Instrument (VI) for stability analysis. The VI was programmed to apply a step of 1 V to the motor, which was a critical step in observing the system's response in terms of servo velocity and position.

With **Figure 9** as our guide, we configured the Simulation Loop to accurately capture the system's behavior over a 2.5-second interval upon the application of the voltage step. This setup allowed us to observe the immediate and subsequent reactions of the servo system to the input.

Figure 10 then offered a visual representation of the system's step response. It allowed us to analyze the system's stability using the Bounded-Input Bounded-Output (BIBO) stability principle. By examining the position and speed responses, we determined the servo system to be stable as it maintained a bounded output for the bounded input provided. This empirical observation aligned with our pole analysis, where we expected a stable response due to poles located in the left-hand plane for the voltage-to-speed system and a marginally stable system for the voltage-to-position system, indicated by poles at zero.

Answering the questions within the lab manual, based on the speed response, we concluded that the system was stable. This matched our results from the pole analysis, confirming that every bounded input yielded a bounded output. Regarding the position response, even though the position continuously increased due to the integral effect of a step input on the position, the system's behavior did not diverge, and thus we could consider it stable within the context of our experiment. The exercise of stopping the VI concluded our stability analysis, providing a comprehensive understanding of the system's reaction to the step input.

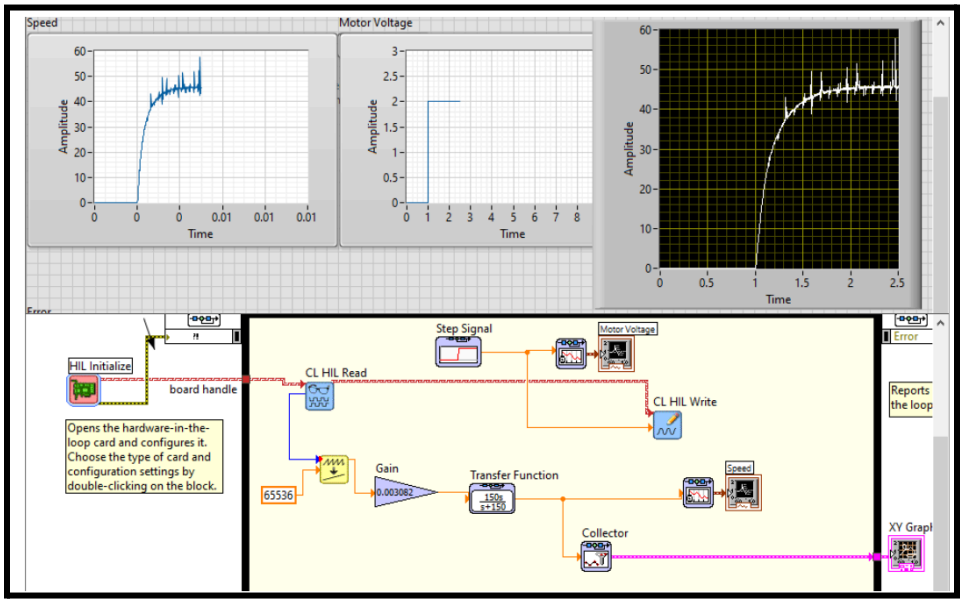

Figure 9:

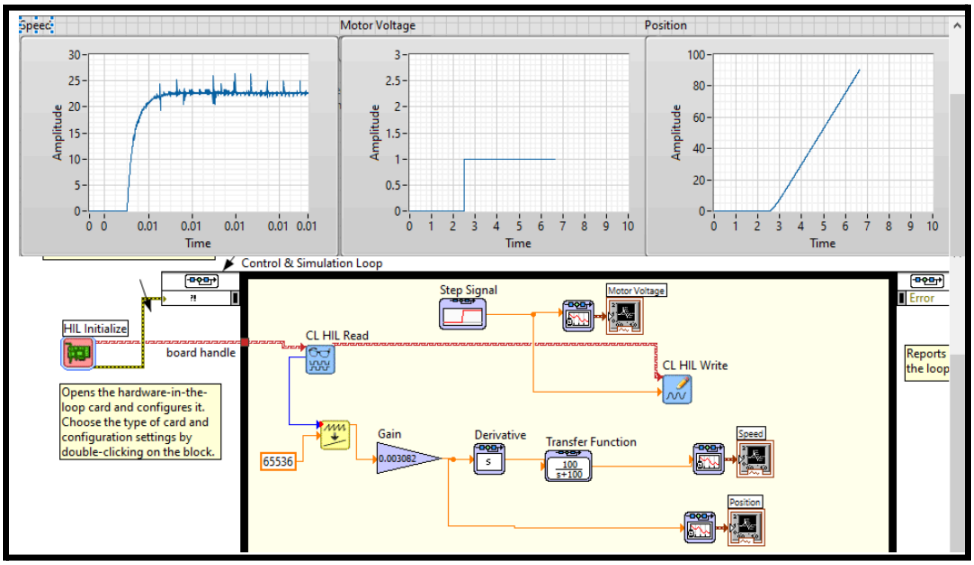

Figure 10:

IV. Bump Test Modeling:

In Part 4 of Experiment 8, focusing on Bump Test Modeling, we set out to apply a 2V step to the motor and read the servo velocity. Using the well-established Virtual Instrument (VI) from previous parts, we initiated the step response test. Within **Figure 11**, we showcased the block

diagram of our VI, designed to implement this test effectively, utilizing the filter values that provided the clearest response earlier.

We then plotted the motor speed response against the input voltage to determine the system's behavior. The data captured in **Figure 12** was particularly crucial for calculating the steady-state gain. By using the cursor feature in the LabVIEW environment, we extracted precise values from the graph to compute the gain.

$$K = \frac{\Delta y}{\Delta u} = \frac{45.1417}{2} = 22.8745$$

Subsequently, we focused on finding the time constant from the observed response, a task depicted in **Figure 13**. This step is essential for characterizing the transient response of our system and for further refining our model.

$$\tau = t_1 - t_0 = 1.27877 - 1 = 278.77\ ms$$

The culmination of our efforts was to validate the model parameters K and τ. We ran the VI with the updated transfer function block, reflecting the first-order model in our equation set. **Figure 14** played a pivotal role here, as it compared the measured response with the simulated response. This comparison aimed to confirm the correctness of our derived parameters.

By analyzing the alignment between the measured and simulated responses, we deduced whether our parameter derivation was accurate. If the simulated response closely followed the measured response, it indicated that our parameters K and τ were indeed derived correctly. We ended Part 4 by stopping the VI, having completed a thorough test of the bump model parameters.

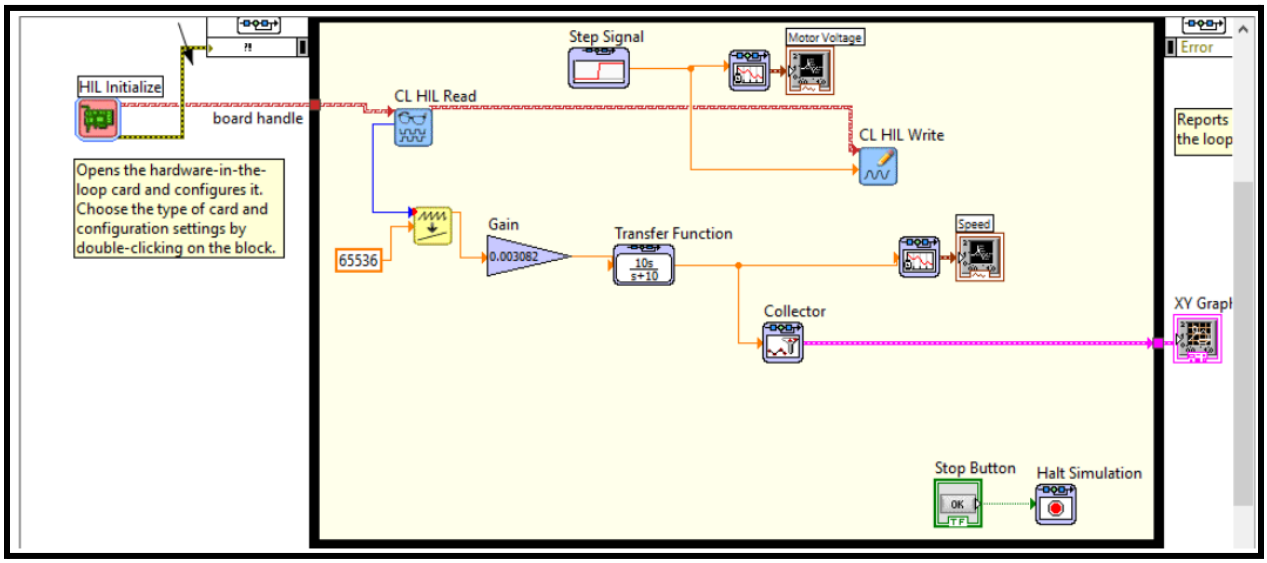

Figure 11: Block Diagram for Bump Test Modeling

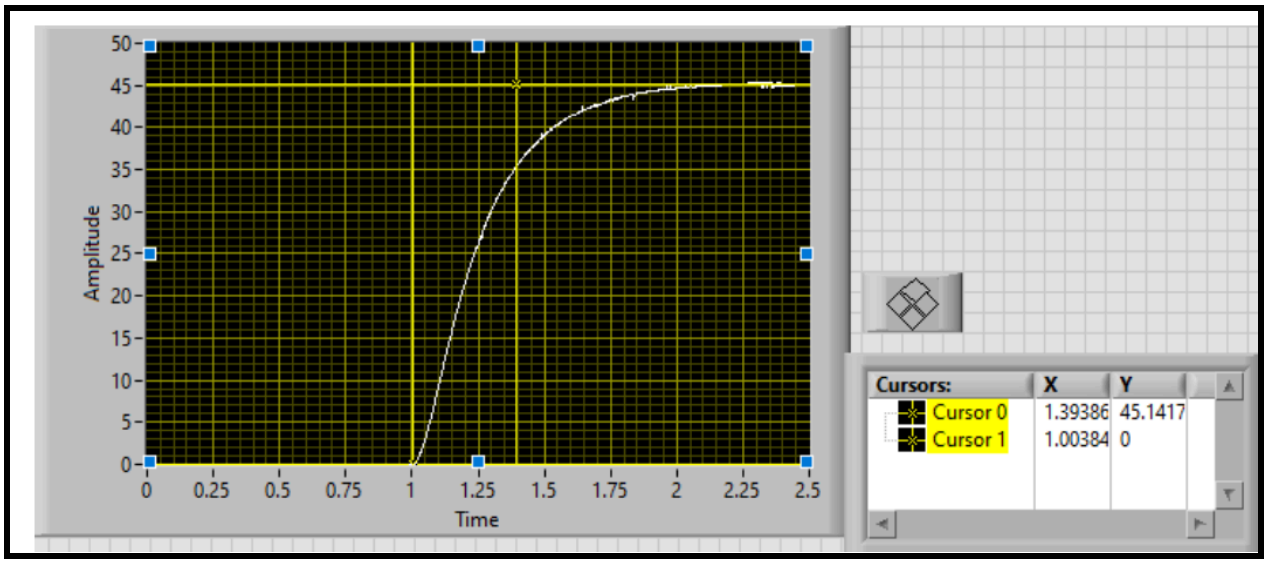

Figure 12: Plot for Steady-State Gain (4.3)

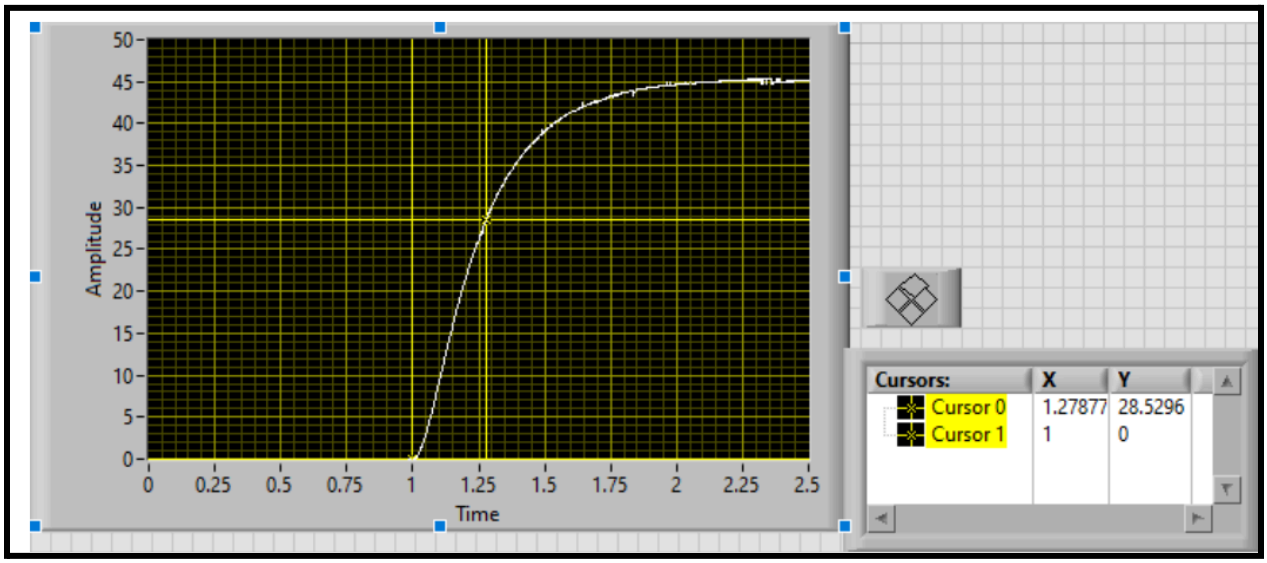

Figure 13: Plot for Time Constant (4.4)

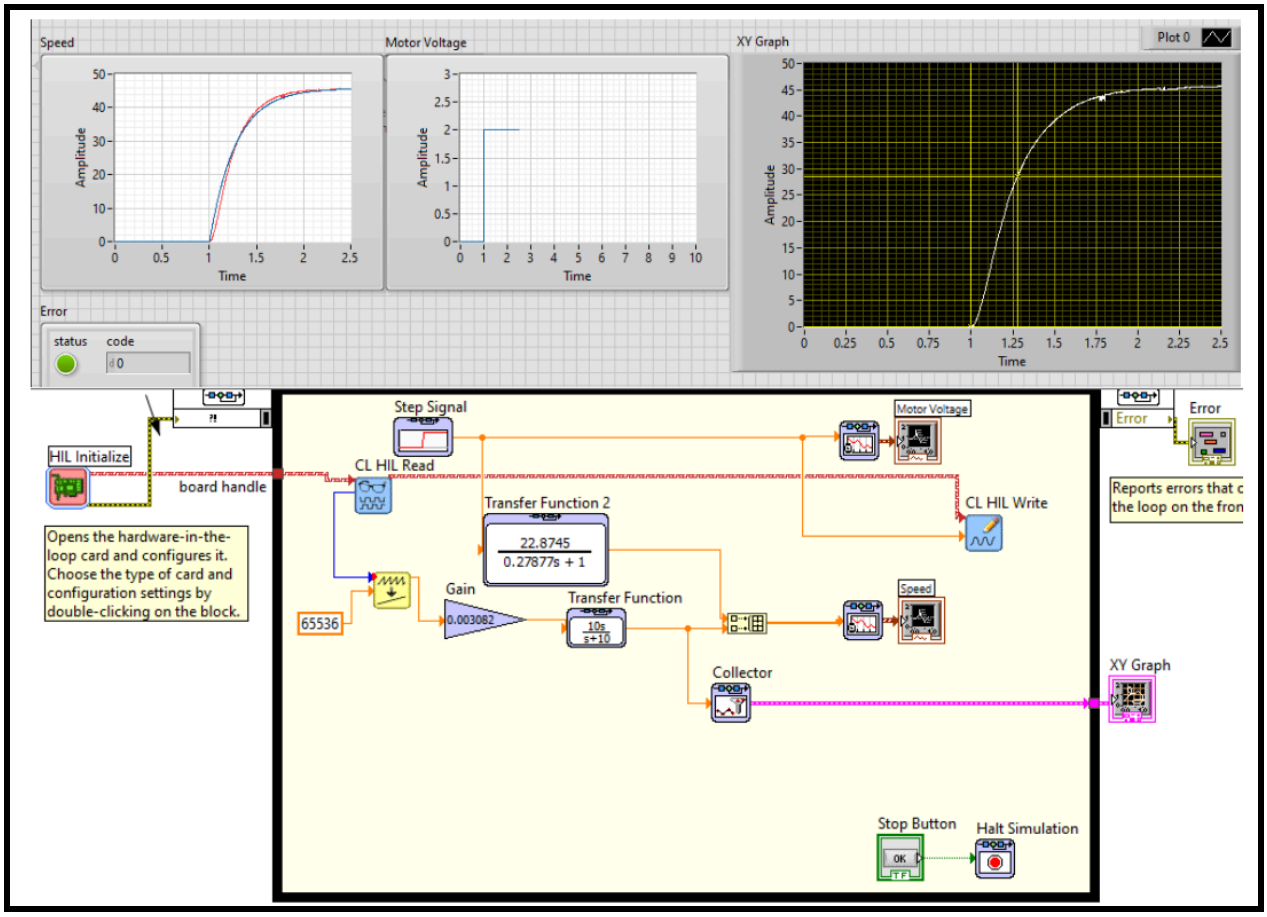

Figure 14: Test for New Gain and Time Constant (4.5).

V. First Principles Modeling:

Following the lab manual, we assembled a simple block diagram that included Gain blocks, a Subtract block, and an Integrator block, which allowed us to transition from acceleration to velocity in our model. The resulting VI, as depicted within **Figure 15**, was then used to apply the 1-3 V 0.4 Hz square wave to the motor.

We ran the VI and observed the response on the waveform chart. The response, illustrated within **Figure 16**, was expected to show whether our model represented the real-world behavior of the QUBE-Servo 2 system. We analyzed the chart to confirm that our simulation mirrored the physical response of the motor to the applied square wave.

$$J_d = \frac{1}{2} m_d r_d^2 = \frac{1}{2}(0.053) * (0.0248)^2 = 16\mu$$

$$J_{eq} = J_m + J_d + J_h = 4 * 10^{-6} + 16 * 10^{-6} + 0.6 * 10^{-6} = 20.6 * 10^{-6}$$

Next, we formulated the differential equation for the motor speed

$$\omega_m J_{eq} R_m + \omega_m K_m^2 - K_m V_m = 0$$

$$\Omega_m J_{eq} R_m + \omega_m K_m^2 = K_m V_m$$

$$\frac{\Omega_m}{V_m} = \frac{K_m}{J_{eq} R_m + \omega_m K_m^2}$$

using the relevant equations provided in the lab manual. This equation was then transformed into the s-domain to obtain the Voltage to Speed transfer function. We compared this function with the results from the Bump Test Modeling to validate the accuracy of our model parameters.

The process of validating our model included ensuring that the measured responses matched the simulated responses under varying conditions. If our model accurately depicted the system's behavior, the responses would be congruent. Finally, we concluded Part 5 by stopping the VI, marking the end of our first principles modeling and confirming the effectiveness of our simulation.

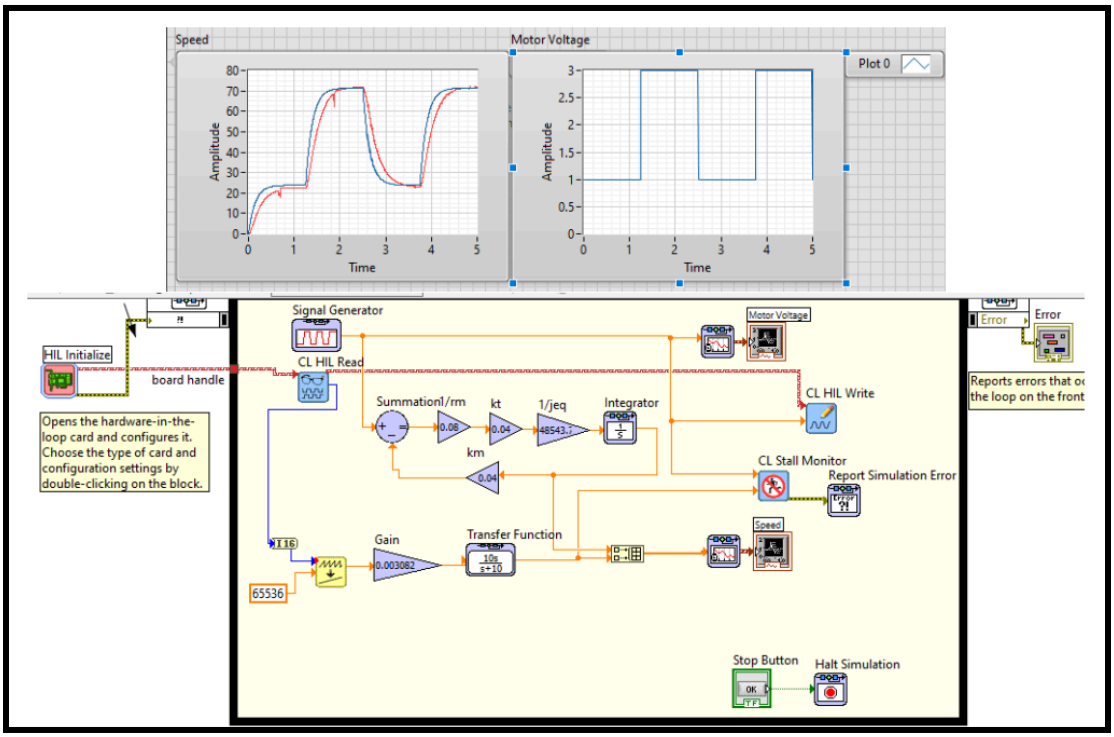

Figure 15: Response for New Block Diagram (5.4)

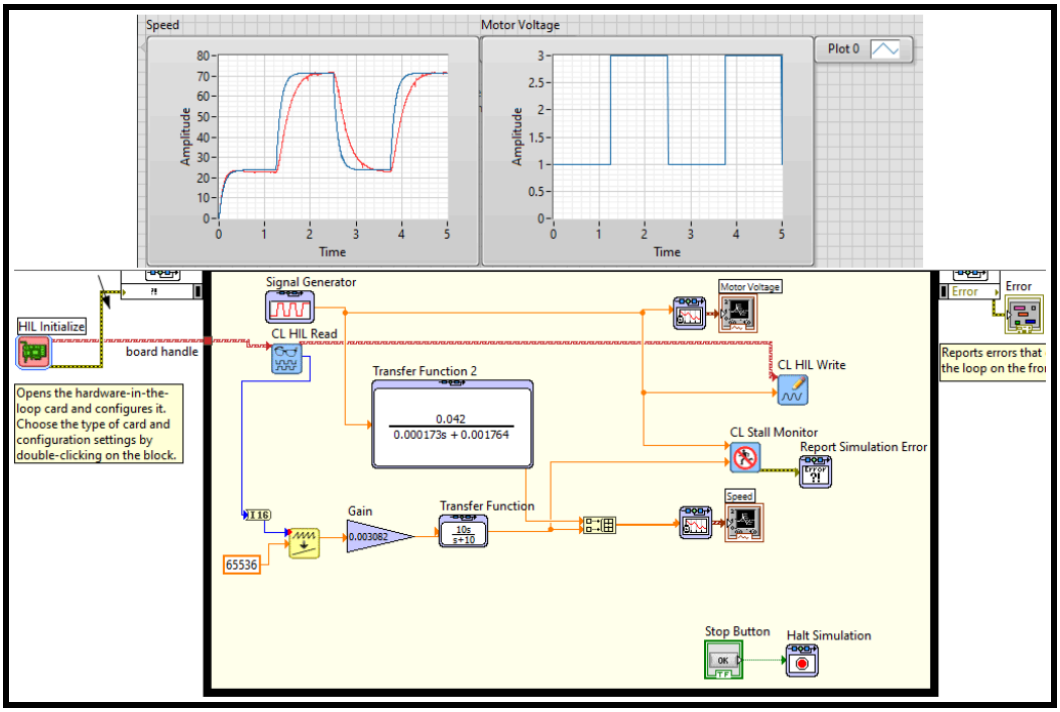

Figure 16: Response for Differential Equation (5.5).

VIII. Conclusion:

As we conclude this laboratory experiment, it is evident that we have gained a profound understanding of the dynamics and control of a servo system. We embarked on this journey by configuring a LabVIEW VI to drive a DC motor and measure its angular position and speed, laying a foundational understanding of the system's basic operation.

Our exploration advanced as we applied filtering techniques to refine the servo velocity measurements. We constructed a VI to implement a low-pass filter that significantly improved the quality of our encoder measurements, which was a pivotal step in achieving accurate system analysis.